Cutting-edge nitrogen, boron, fluorine triply doped chain-like porous carbon nanofibers: a versatile solution for high-performance zinc-air batteries and self-powered water splitting

Alagan Muthurasu[1], Ishwor Pathak[1], Debendra Acharya[1], Yagya Raj Rosyara [1], Hak Yong Kim[1,2*]

[1]Department of Nano Convergence Engineering, Jeonbuk National University, Jeonju 561-756, Republic of Korea
[2]Department of Organic Materials and Fiber Engineering, Jeonbuk National University, Jeonju 561-756, Republic of Korea
Corresponding Author's E-mail: khy@jbnu.ac.kr,

1.2 Tafel calculation:

The kinetic current of the RDE mass-transport correction was measured in the Tafel plot by:

$$J_K = \frac{J \times J_L}{J - J_L} \qquad (4)$$

Where J, is the calculated current density, J_L and J_K are the kinetics and diffusion-limited current density, respectively.

1.3 Zn–air battery performance calculation:

The following formula was used to calculate the specific capacity.

$$Specific\ capacity = \frac{current\ \times service\ hour}{weight\ of\ consumed\ zinc} \qquad (5)$$

The following formula was used to calculate the energy density.

$$Energy\ density = \frac{current\ \times service\ hour \times avearge\ discharge\ voltage}{weight\ of\ consumed\ zinc} \qquad (6)$$

In this study, the crosslinked PVA-BA-PTFE will be converted into B-doped PCNFs. Based on the reaction:

$$2B(s) + N_2(g) = 2BN(s)$$

Where N_2: $\Delta fHm = 0$ Kj mol^{-1} ; $\Delta fGm = 0$ Kj mol^{-1} ; $Sm = 191.5$ J mol^{-1} K^{-1} ;

B: $\Delta fHm = 0$ Kj mol^{-1} ; $\Delta fGm = 0$ Kj mol^{-1} ; Sm = 5.86 J mol-1 K^{-1} ;

BN: $\Delta fHm = -254.39$ Kj mol^{-1} ; $\Delta fGm = -228.45$ Kj mol^{-1} ; $Sm = 14.81$ J mol^{-1} K^{-1} ;

Therefore, for this reaction, $\Delta H = -254.39$ Kj mol^{-1} ; $\Delta S = -86.8$ J mol^{-1} K^{-1} ; $\Delta G = -228.4$ kJ $mol^{-1} < 0$,

Based on the Gibbs function, the reaction between B and N_2 is considered spontaneous when the value of ΔG is less than zero. This implies that the reaction can occur at room temperature. However, it should be noted that high temperatures can speed up the reaction process.

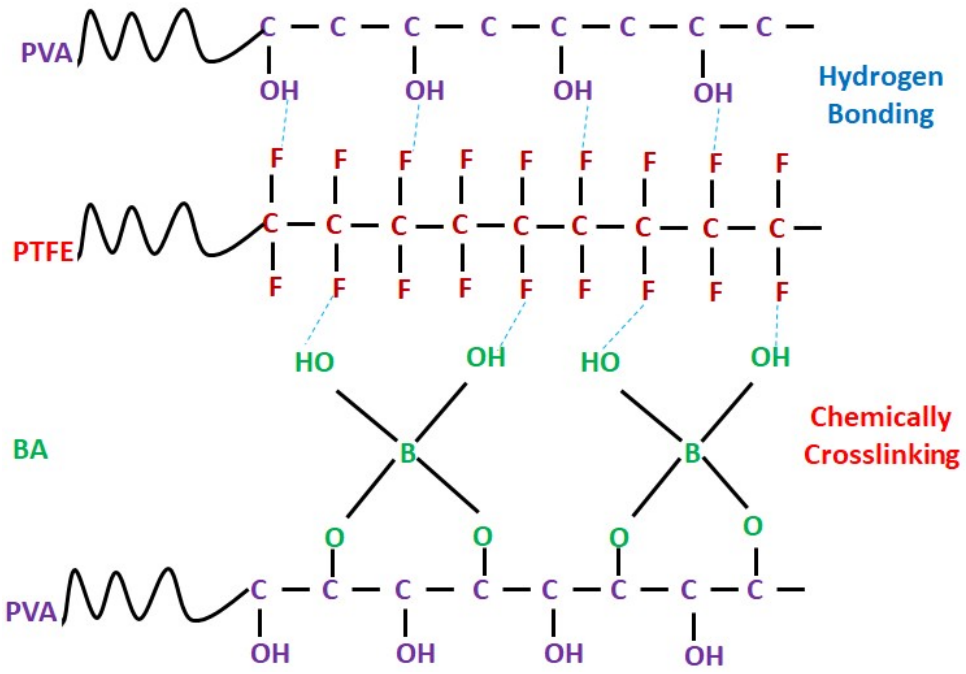

Figure S1. A schematic diagram of chemical crosslinking electrospinning to synthesize as-spun fibers.

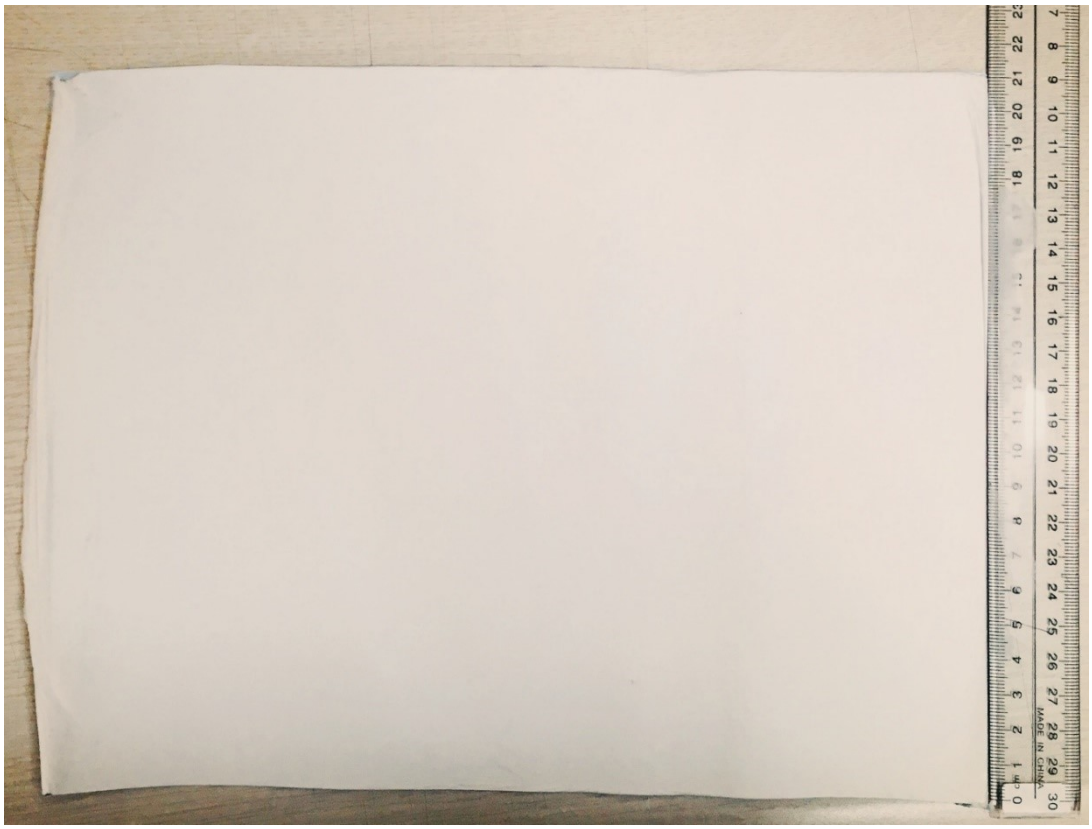

Figure S2. A digital photographic image of the as-spun film with a size of 25 cm × 20 cm

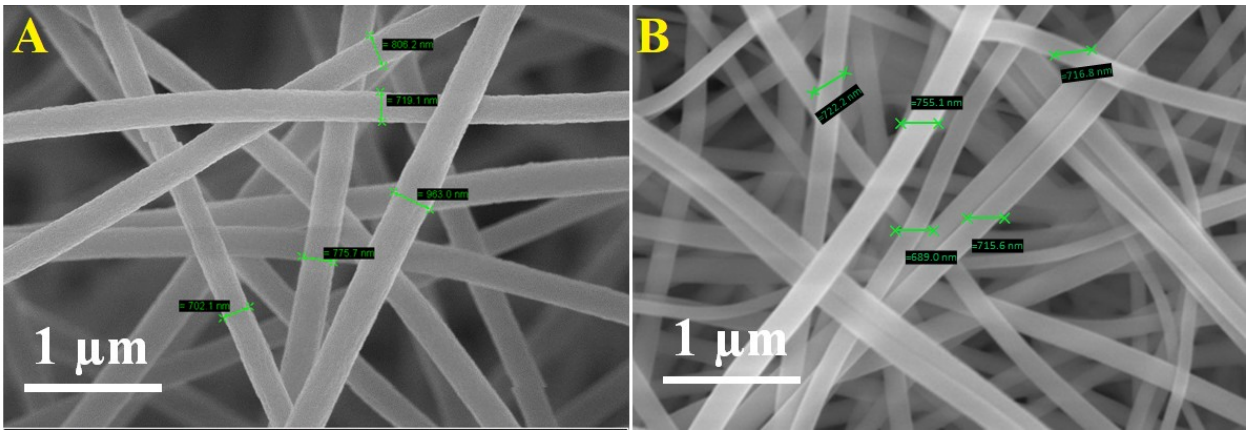

Figure S3. FESEM image of the as-spun (A) PVA and (B) PVA: PTFE fiber.

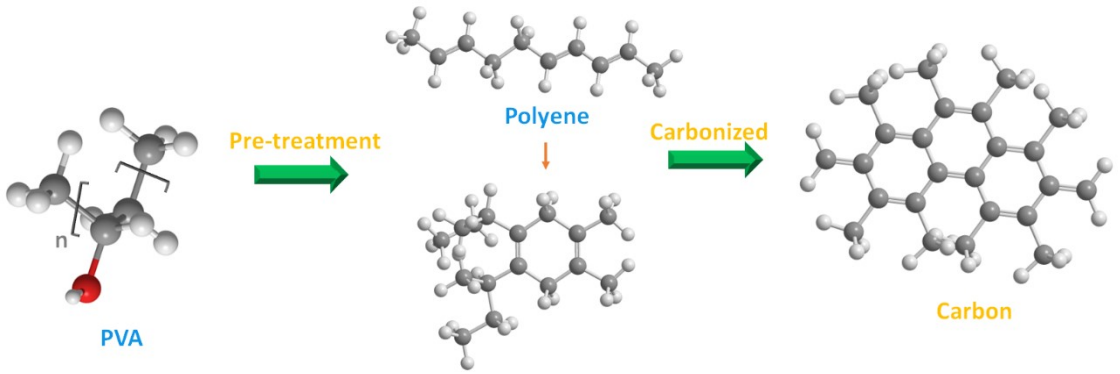

Figure S4. Potential PVA activity after the heat treatment method.

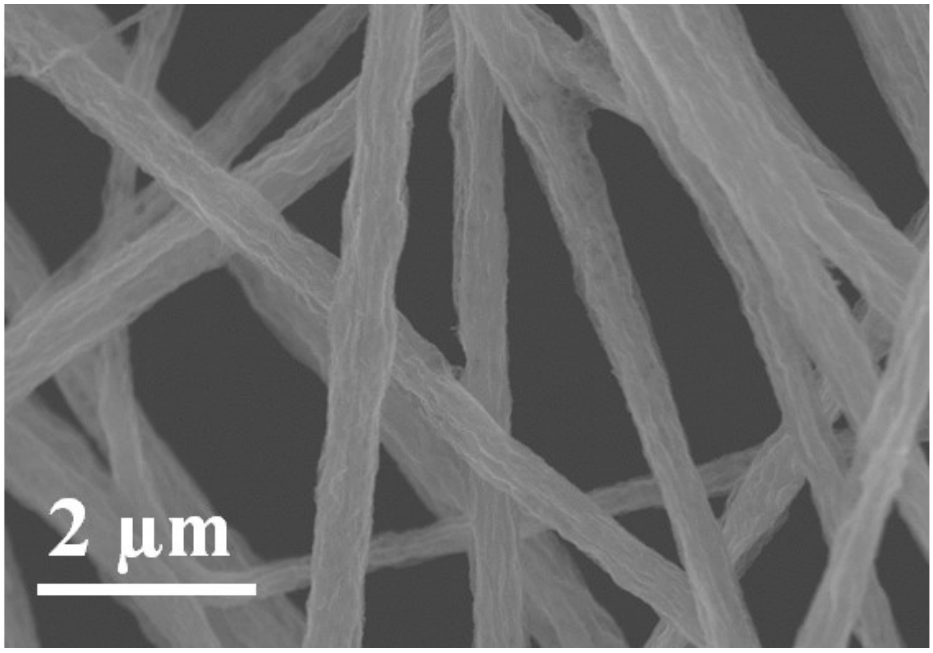

Figure S5. FESEM image of the PVA: PTFE oxidized fiber.

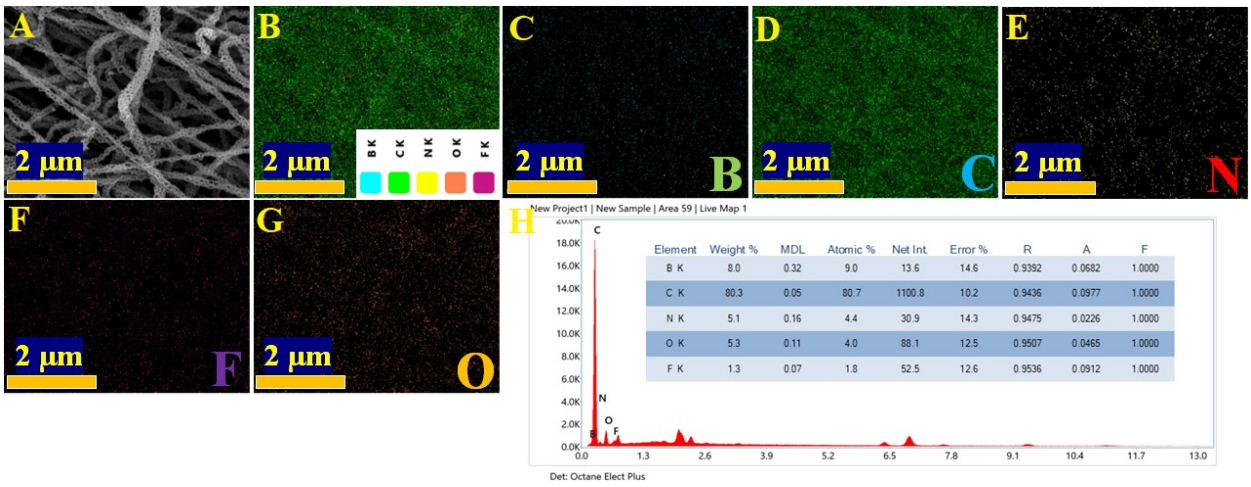

Figure S6. (A) FESEM, (B-G) elemental mapping, and (H) EDX spectrum and inset image corresponding elemental compositions of N, B, and F-doped PCNFs.

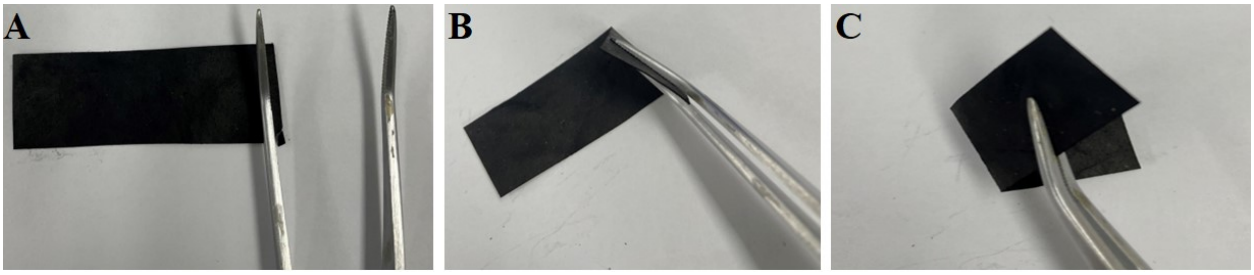

Figure S7. Digital photograph of repeated bending of N, B, and F-doped PCNFs.

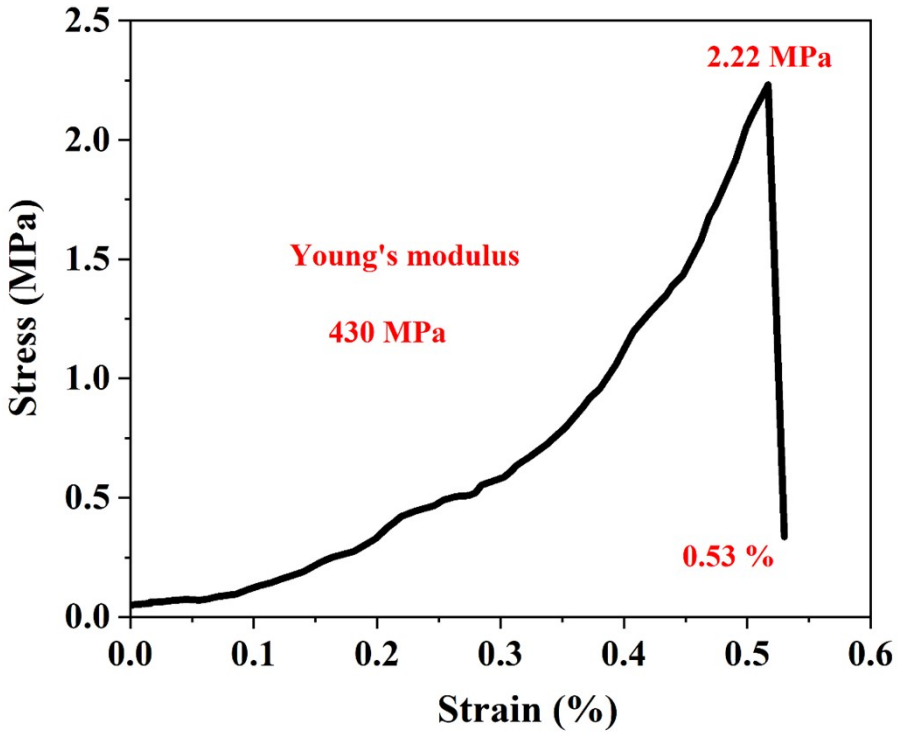

Figure S8. Tensile stress–strain curve of the N, B, and F-doped PCNFs film that was made at 1200 °C.

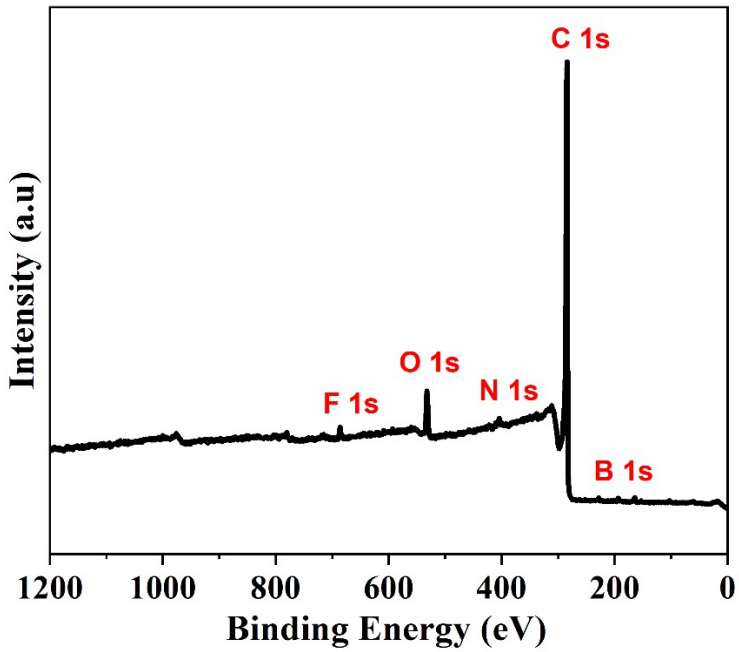

Figure S9. XPS survey spectrum of N, B, and F-doped PCNFs.

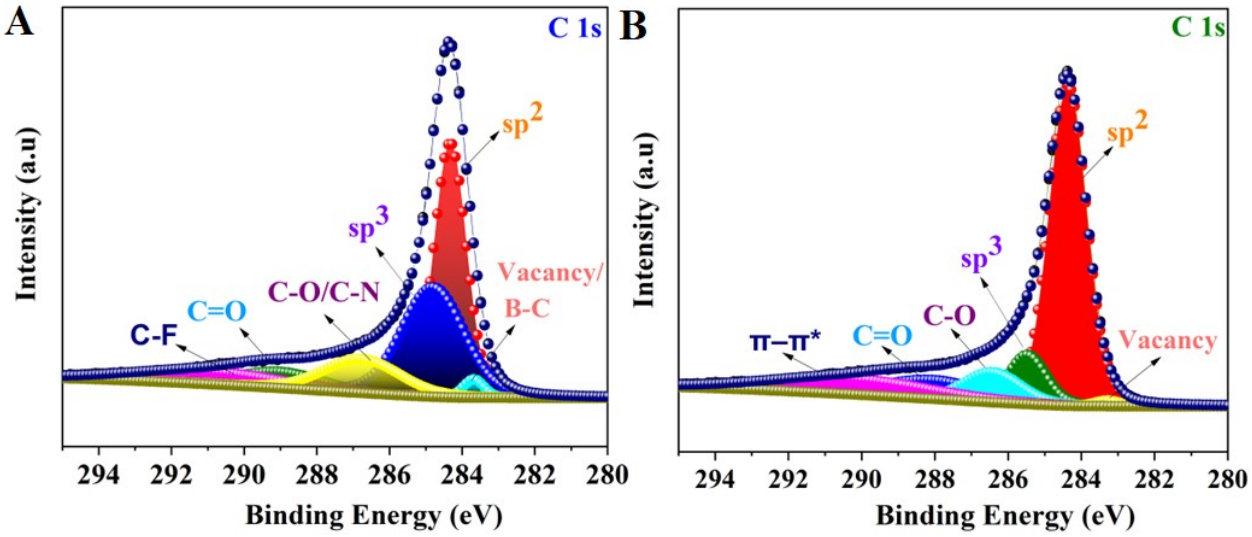

Figure S10. High-resolution C 1s XPS spectra of (A) N, B, and F-doped PCNFs, and (B) CNFs respectively.

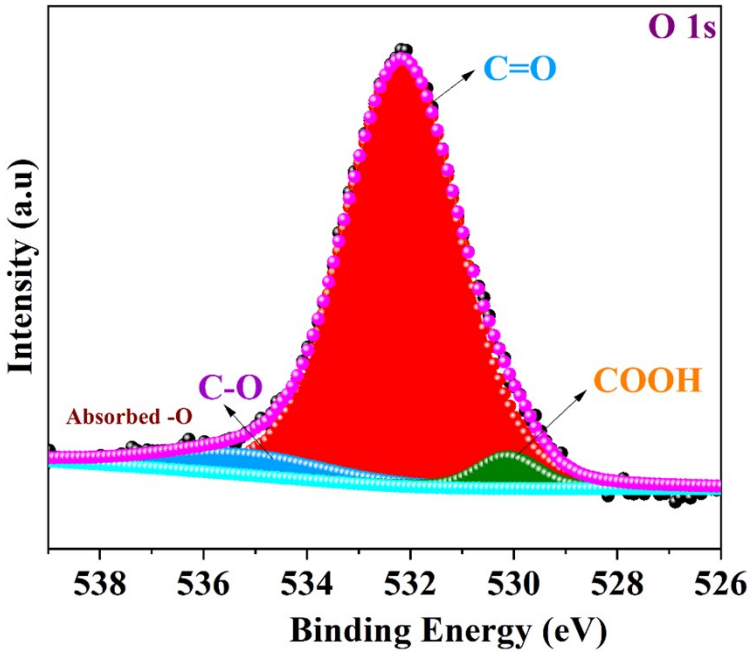

Figure S11. High-resolution O1s XPS spectra of N, B, and F-doped PCNFs.

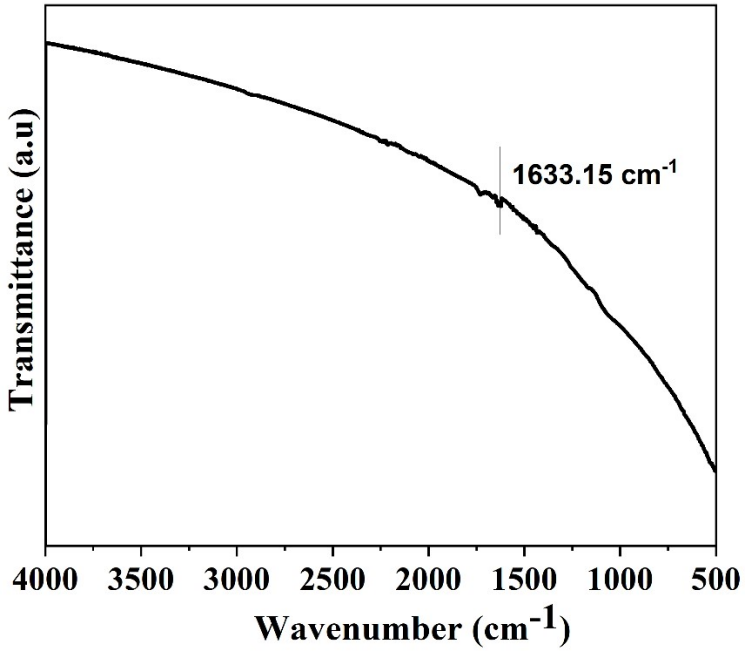

Figure S12. FTIR spectrum of N, B, and F-doped PCNFs at 1200 °C.

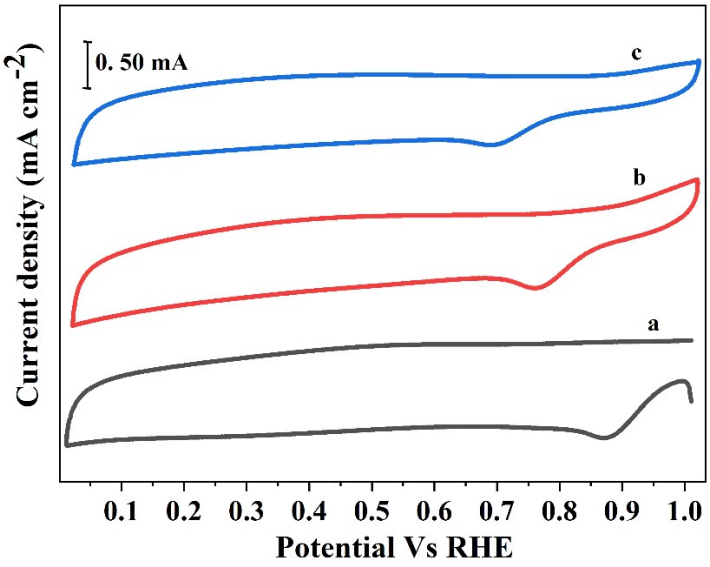

Figure S13. CV curves of N, B, and F-doped PCNFs in 0.1 M KOH (a), 0.5 M H_2SO_4 (b) and 0.01 M PBS electrolytes, respectively.

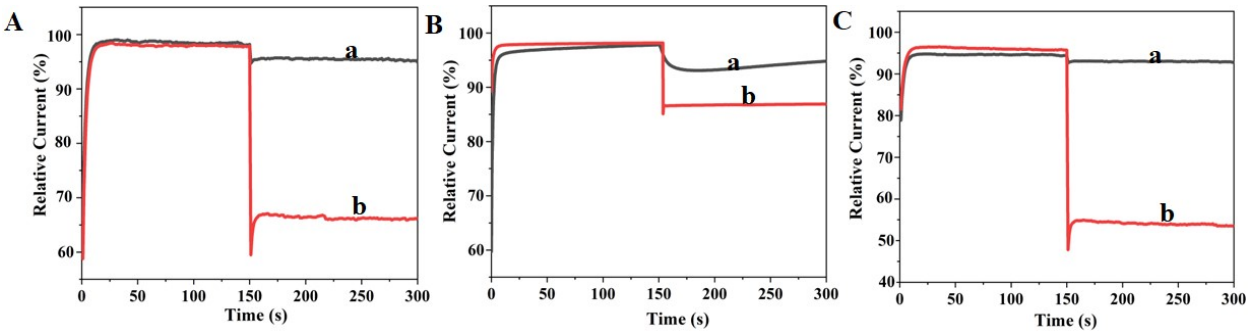

Figure S14. Current-time (i-t) chronoamperometric curves of N, B, and F-doped PCNFs (a) and Pt/C (b) with the addition of methanol (3 wt%) at a rotation rate of 1600 rpm on the RDE in 0.1 M KOH (A), 0.5 M H_2SO_4 (B) and 0.01 M PBS (C) electrolytes.

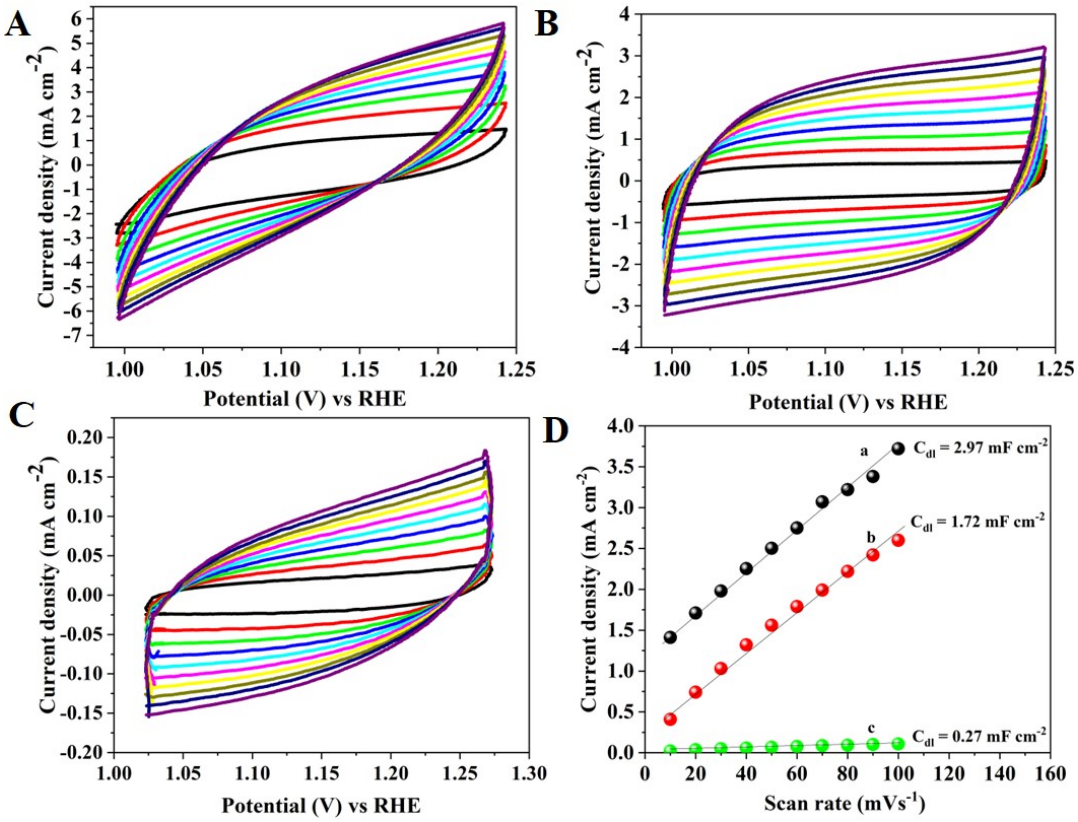

Figure S15. CVs of (A) N, B, and F-doped PCNFs, (B) CNF, and (C) GCE at various scan rates in 1.0 M KOH and (D) linear fitting of sweep rates with capacitive current densities for (a) N, B, and F-doped PCNFs, (b) CNF, and (c) GCE catalysts.

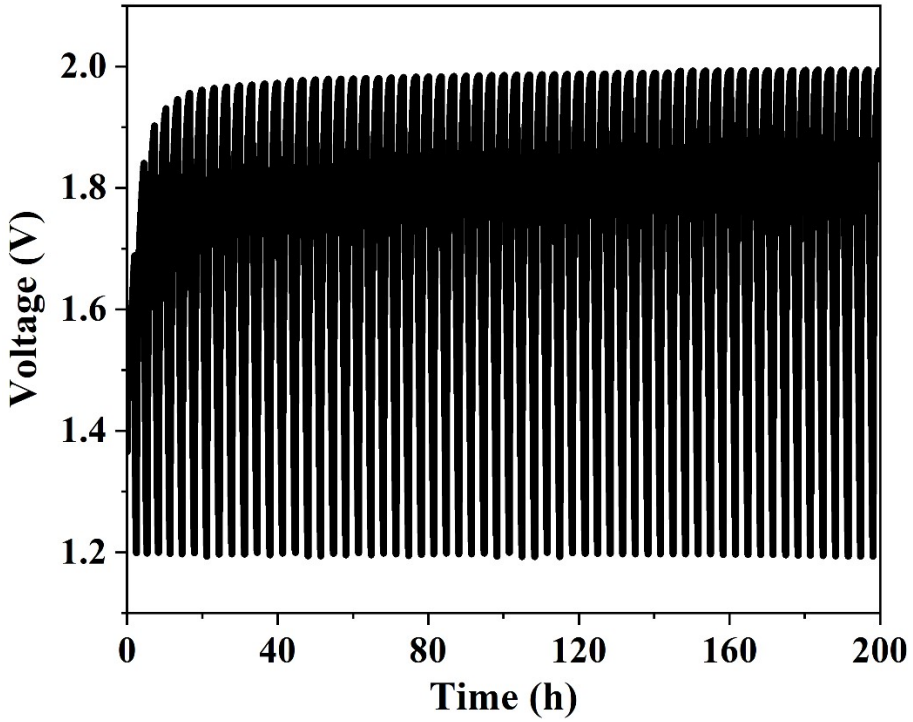

Figure S16. Galvanostatic charge and discharge test of N, B, and F-doped PCNFs-based liquid Zn-air batteries at 5 mA cm^{-2}.

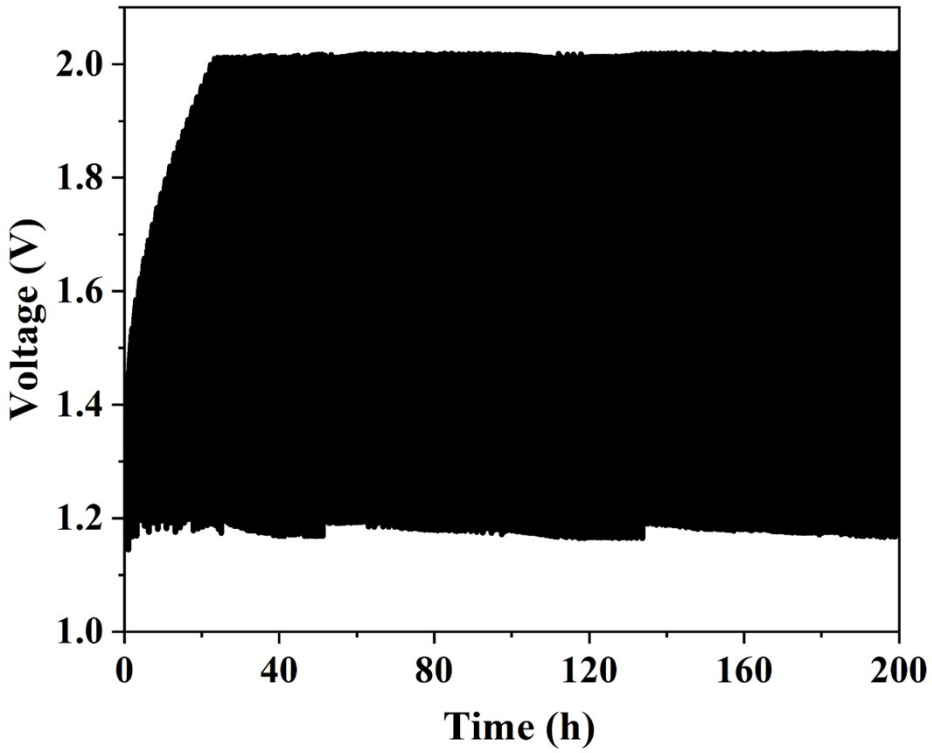

Figure S17. Galvanostatic charge and discharge test of N, B, and F-doped PCNFs-based liquid Zn-air batteries at 10 mA cm^{-2}.

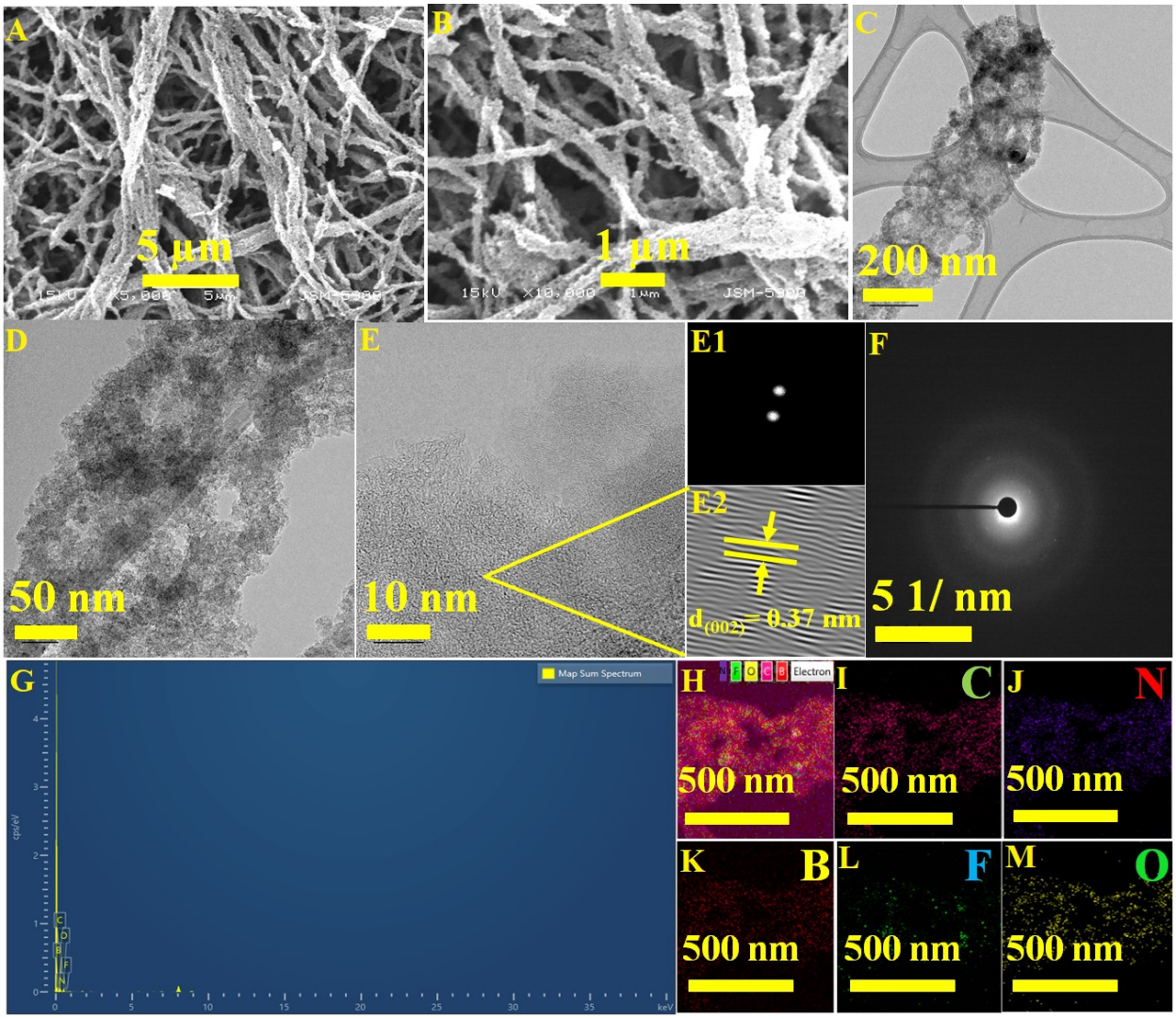

Figure S18. (A-B) SEM, (C-D) TEM, (E) HRTEM, (E1) images fast Fourier transfer (FFT) of the area before and after applying the mask, (E2) the inverse fast Fourier transfer (iFFT), (F) SAED pattern, (G) EDX spectrum and (H-O) elemental mapping images of N, B, and F-doped PCNFs after charge and discharge test.

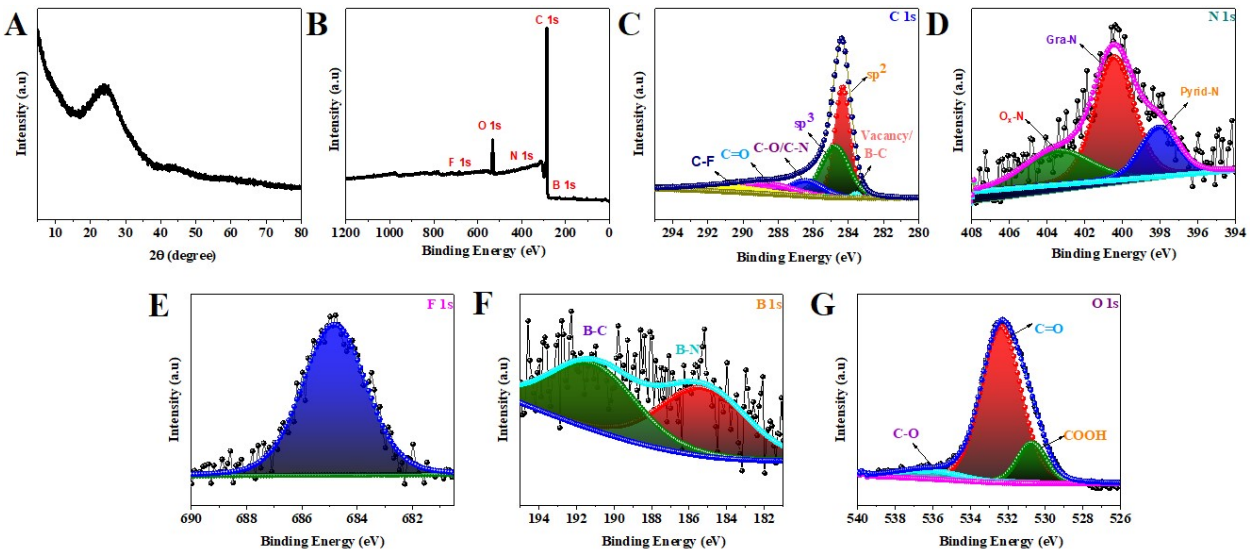

Figure S19. (A) XRD patterns, (B) XPS survey spectrum, high-resolution XPS spectra of (C) C 1s, (D) N 1s, (E) F 1s, (F) B 1s, and (G) O 1s for N, B, F-doped PCNFs after charge and discharge test.

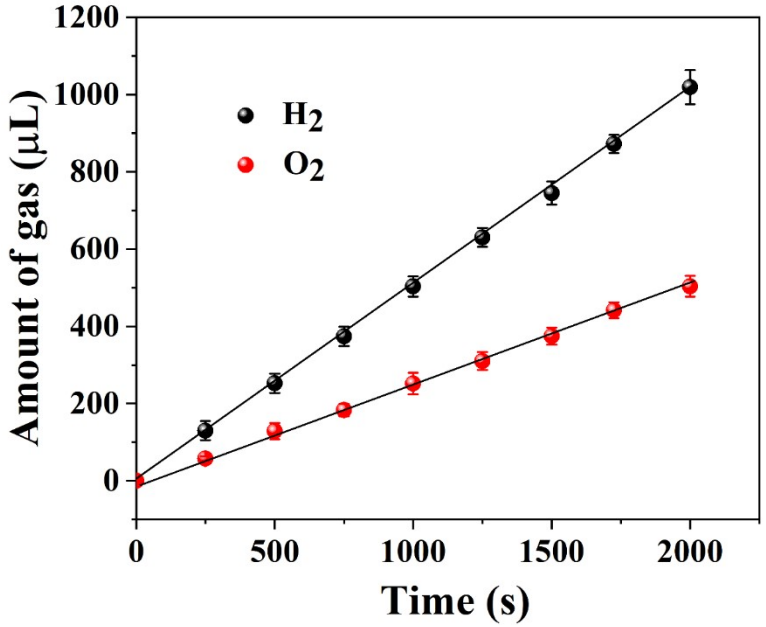

Figure S20. Volumes of H_2 and O_2 are produced as a function of water-splitting time.

Sample	Vacancy /C_{total} (%)	sp^2 / C_{total} (%)	Sp^3 / C_{total} (%)	C-O /C_{total} (%)	C=O /C_{total} (%)	π-π* /C_{total} (%)
N, B, F-doped PCNFs	4.7	40.1	29.6	15.4	9.9	5.8
CNFs	1.7	60.2	10.3	8.5	9.4	4.8

Table S1: The surface carbon species level in N, B, and F-doped PCNFs and CNFs samples were evaluated using high-resolution C1s XPS spectra.

Table S2: The electrocatalytic ORR activity of recently published metal-free ORR catalysts in 0.1M KOH solutions.

Sample	**Electrolyte**	**E_{onset} (V)**	**ORR $E_{1/2}$ (V)**	**Ref**
NPC@CNF-950	0.1 M KOH	0.85	0.88 V	S1
MWCNTs	0.1 M KOH	0.92	0.8	S2
GO	0.1 M KOH	0.82	-	S3
BNPC-1100	0.1 M KOH	0.894	0.793	S4
NBC-1000	0.1 M KOH	0.97	0.84	S5
B-OLC-1-20	0.1 M KOH	0.80	-	S6
N, P-GC-1000	0.1 M KOH	1.02	0.85	S7
N, F-MCFs-A	0.1 M KOH	0.94	0.81	S8
FCNPs	0.1 M KOH	1.0	-	61
N-HsGDY	0.1 M KOH	1.02	0.85	S9
GSP-1000	0.1 M KOH	1.03	0.85	S10
N, B, and F-doped PCNFs	**0.1 M KOH** **0.5 M H_2SO_4** **0.01 M PBS**	**0.99** **0.90** **0.82**	**0.90** **0.79** **0.70**	**This work**

Table S3: Comparison of the OER activity for various recently reported highly heteroatom doped metal-free catalysts in 1 M KOH solution.

Sample	**Overpotential (@ 10 mA cm^{-2})**	**Tafel slope ($mV\ dec^{-1}$)**	**Electrolyte**	**Ref**
NSCG	310 mV	65	1 M KOH	S11
N, S, O carbon nanosheet	420 mV	53	1 M KOH	S12
N, P-carbon paper	420 mV	61.6	1 M KOH	S13
NGSHs	420 mV	83	1 M KOH	S14
N-doped graphitic carbon	380 mV	-	1 M KOH	S15
BNPC-1100	570 mV	201	1 M KOH	S4
N, P-GC-1000	330 mV	67	1 M KOH	S7
40F-KB	370 mV	-	1 M KOH	62
LC-KOH	470 mV	105.1	1 M KOH	S16
N, S-CNT	360 mV	56	1 M KOH	S17
O-CNT	360 mV	47.7	1 M KOH	S18
N, B, and F-doped PCNFs	**280 mV** **913 mV**	**87** **96**	**1.0 M KOH** **0.5 M H_2SO_4**	**This work**

Table S4: A comparison study of carbon-based rechargeable Zn-air batteries using liquid alkaline electrolytes.

Sample	**OCP (V)**	**Power density /mW cm^{-2}**	**Specific capacity /mA h g_{zn}^{-1}**	**Ref**
NSCG	1.34	5.9 mW cm^{-2}	-	S11
TD-CFs	1.46	-	-	23
2D-PPCN	1.40	-	555 mA h g_{zn}^{-1}	S19
NPCS-900	1.40	55 mW cm^{-2}	432 mA h g_{zn}^{-1}	S20
NDGs-800	1.45	115.2 mW cm^{-2}	-	S21
NPS-G-2	1.372	151 mW cm^{-2}	686 mA h g_{Zn}^{-1}	12
BN/C	1.36	115 mW cm^{-2}	802 W h kg_{Zn}^{-1}	S22
o-CC-H_2	-	91.4 mW cm^{-2}	707 mAh g^{-1}	S23
NCN-1000-5	1.44	207 mW cm^{-2}	672 mA h g^{-1}	S24
O–N–CNs	1.49	89 mW cm^{-2}	660 mAh g^{-1}	S25
N-CNF	1.50	-	615 mAh g^{-1}	S26
N, B, and F-doped PCNFs	**1.453**	**151.9 mW cm^{-2}**	**729 mA h g_{zn}^{-1}**	**This work**

References

S1 Y. Li, M. Chen, M. Chu, X. Wang, Y. Wang, X. Lin and X. Cao, *ChemElectroChem*, 2021, **8**, 829–838.

S2 Y. Pei, H. Song, Y. Liu, Y. Cheng, W. Li, Y. Chen, Y. Fan, B. Liu and S. Lu, *J. Colloid Interface Sci.*, 2021, **600**, 865–871.

S3 M. Zhang, H. Tao, Y. Liu, C. Yan, S. Hong, J. Masa, A. W. Robertson, S. Liu, J. Qiu and Z. Sun, *ACS Sustain. Chem. Eng.*, 2019, **7**, 3434–3442.

S4 Y. Qian, Z. Hu, X. Ge, S. Yang, Y. Peng, Z. Kang, Z. Liu, J. Y. Lee and D. Zhao, *Carbon N. Y.*, 2017, **111**, 641–650.

S5 Y. Zhou, Y. Sun, H. Wang, C. Zhu, J. Gao, D. Wu, H. Huang, Y. Liu and Z. Kang, *Inorg. Chem. Front.*, 2018, **5**, 2985–2991.

S6 Y. Lin, Y. Zhu, B. Zhang, Y. A. Kim, M. Endo and D. S. Su, *J. Mater. Chem. A*, 2015, **3**, 21805–21814.

S7 Z. Zhou, A. Chen, X. Fan, A. Kong and Y. Shan, *Appl. Surf. Sci.*, 2019, **464**, 380–387.

S8 T. Gong, R. Qi, X. Liu, H. Li and Y. Zhang, *Nano-Micro Lett.*, 2019, **11**, 1–11.

S9 Q. Lv, W. Si, J. He, L. Sun, C. Zhang, N. Wang, Z. Yang, X. Li, X. Wang, W. Deng, Y. Long, C. Huang and Y. Li, *Nat. Commun.*, 2018, **9**, 3376.

S10 B. Huang, Y. Liu, X. Huang and Z. Xie, *J. Mater. Chem. A*, 2018, **6**, 22277–22286.

S11 S. Chen, J. Duan, Y. Zheng, X. Chen, X. W. Du, M. Jaroniec and S. Z. Qiao, *Energy Storage Mater.*, 2015, **1**, 17–24.

S12 K. Qu, Y. Zheng, S. Dai and S. Z. Qiao, *Nano Energy*, 2016, **19**, 373–381.

S13 T. Y. Ma, J. Ran, S. Dai, M. Jaroniec and S. Z. Qiao, *Angew. Chemie - Int. Ed.*, 2015, **54**, 4646–4650.

S14 G. L. Tian, M. Q. Zhao, D. Yu, X. Y. Kong, J. Q. Huang, Q. Zhang and F. Wei, *Small*, 2014, **10**, 2251–2259.

S15 Y. Zhao, R. Nakamura, K. Kamiya, S. Nakanishi and K. Hashimoto, *Nat. Commun.*, 2013,

4, 2390.

S16 M. Devi, C. Madan, A. Halder and S. Sharma, *Carbon Trends*, 2022, **9**, 100221.

S17 K. Qu, Y. Zheng, Y. Jiao, X. Zhang, S. Dai and S. Z. Qiao, *Adv. Energy Mater.*, 2017, **7**, 1602068.

S18 L. Li, H. Yang, J. Miao, L. Zhang, H. Y. Wang, Z. Zeng, W. Huang, X. Dong and B. Liu, *ACS Energy Lett.*, 2017, **2**, 294–300.

S19 W. Lei, Y. P. Deng, G. Li, Z. P. Cano, X. Wang, D. Luo, Y. Liu, D. Wang and Z. Chen, *ACS Catal.*, 2018, **8**, 2464–2472.

S20 S. Chen, L. Zhao, J. Ma, Y. Wang, L. Dai and J. Zhang, *Nano Energy*, 2019, **60**, 536–544.

S21 Q. Wang, Y. Ji, Y. Lei, Y. Wang, Y. Wang, Y. Li and S. Wang, *ACS Energy Lett.*, 2018, **3**, 1183–1191.

S22 R. Zhao, Q. Li, Z. Chen, V. Jose, X. Jiang, G. Fu, J. M. Lee and S. Huang, *Carbon N. Y.*, 2020, **164**, 398–406.

S23 H. F. Wang, C. Tang, B. Wang, B. Q. Li, X. Cui and Q. Zhang, *Energy Storage Mater.*, 2018, **15**, 124–130.

S24 H. Jiang, J. Gu, X. Zheng, M. Liu, X. Qiu, L. Wang, W. Li, Z. Chen, X. Ji and J. Li, *Energy Environ. Sci.*, 2019, **12**, 322–333.

S25 J. J. Lv, Y. Li, S. Wu, H. Fang, L. L. Li, R. Bin Song, J. Ma and J. J. Zhu, *ACS Appl. Mater. Interfaces*, 2018, **10**, 11678–11688.

S26 H. W. Liang, Z. Y. Wu, L. F. Chen, C. Li and S. H. Yu, *Nano Energy*, 2015, **11**, 366–376.